arXiv:physics/0508038v2 [physics.atom-ph] 29 Sep 2005

Parity nonconservation in Atomic Zeeman Transitions

E.J. Angstmann, T.H. Dinh, and V.V. Flambaum
School of Physics, University of New South Wales, Sydney 2052, Australia

(Dated: February 2, 2008)

We discuss the possibility of measuring nuclear anapole moments in atomic Zeeman transitions and perform the necessary calculations. Advantages of using Zeeman transitions include variable transition frequencies and the possibility of enhancement of parity nonconservation effects.

PACS numbers: 32.80.Ys, 32.60.+i, 24.80.+y

Experiments on parity nonconservation in atoms have measured the electron-nucleon weak interaction and have provided very accurate tests of the Standard Model at low energies (see, e.g., review [1]). It has been pointed out in Ref. [2] that atomic experiments can be used to measure the nuclear anapole moment and study parity nonconserving (PNC) nuclear forces. The measurement of the anapole moment of ^{133}Cs nucleus was reported in Ref. [3]. However, the strength of the PNC nuclear forces extracted from this measurement seem to disagree with the limits on these forces extracted from the ^{205}Tl anapole measurement performed in another atomic experiment [4]. Moreover, the general situation with PNC nuclear forces at the moment is controversial since different experiments give contradictory results (see, e.g., review [1]). This situation requires new measurements of nuclear anapole moments.

The PNC interaction in atoms can be split into a nuclear spin-dependent (NSD) and nuclear spin-independent (NSI) part. The NSI part is due to the nuclear weak charge, and the PNC effects produced by the NSI part are two orders of magnitude larger than the PNC effects produced by the NSD part. There are three contributions to the NSD part of the PNC interaction: the nuclear anapole moment, the NSD part of the electron-nucleus interaction, and the combination of the NSI electron-nucleus weak interaction and the hyperfine interaction. For heavy atoms the anapole moment contribution dominates since it grows as $A^{2/3}$[2, 5, 6]. In experiments [3, 4] the NSD contribution was separated from the much larger NSI contribution. The NSD contribution is different in different hyperfine components of an optical transition and can be extracted from the difference of the PNC effects in these components. An alternative method to measure the NSD interaction was suggested in Ref. [7]. The NSI part is zero in transitions between hyperfine terms of a ground state electronic level. The measurements of PNC in the hyperfine transitions is sensitive to the NSD PNC interaction only. Unfortunately, no such experiment has been performed.

It was suggested in Refs. [8] (see also review [9] and references therein) that the transitions between the Zeeman components of the hyperfine levels of a ground state atom in a magnetic field may be more convenient for the measurements of PNC induced by the NSD interaction, than transitions between the hyperfine levels themselves. The NSI interaction still does not contribute here, therefore, the measurement of the PNC effects in Zeeman transitions can provide a value of the nuclear anapole moment. One advantage of using these transitions is that for weak external magnetic fields, the transition frequency is proportional to the field and so can be chosen arbitrarily small, and determined from the conditions required for optimal experimental setup. Advantages of the low frequency were explained in the proposal of possible experiments in hydrogen, potassium and cesium hyperfine transitions [10]. At low frequencies one does not need a resonator to produce the electromagnetic field. This greatly simplifies the experiment and allows the frequency to be set to the same value for different atoms. It should be noted that the PNC E1 amplitudes of the Zeeman transitions in weak magnetic fields are suppressed by a factor $\hbar\omega/\Delta E_{hf}$, where ω is the transition frequency and ΔE_{hf} is the hyperfine splitting. However, the E1 amplitude increases with nuclear charge as $d \propto Z^2 A^{2/3} R_a$, where R_a is a relativistic correction factor (see, e.g. [1, 11]), while the hyperfine splitting increases as $\Delta E_{hf} \propto Z$. Combining these results we can see that the E1 amplitude of Zeeman transitions increases faster than $ZA^{2/3}$ for heavy atoms in weak magnetic fields at a fixed transition frequency. This suggests that heavy atoms should be considered as candidates for an experiment.

Another possible advantage appears for Zeeman transitions in a strong magnetic field [8, 10]. Parity nonconservation appear due to interference between the PNC electric dipole amplitude, d, and the magnetic dipole amplitude, μ, $P \sim Im[2d\mu/(|\mu|^2 + |d|^2)] \approx 2Im(d/\mu)$. In a strong magnetic field an eigenstate is approximately a product of the nuclear spin state times the electron wave function. The $M1$ amplitude, μ, between the Zeeman states corresponding to nuclear spin-flip is very small, since the nuclear magnetic moment is ∼1000 times smaller than the electron magnetic moment (in reality the contribution from the small admixture of the state with a different electron angular momentum projection will always dominate μ). The magnitude of the PNC amplitude, d, is not suppressed for such transitions. This enhances the value of PNC effects ($\sim d/\mu$) containing μ in the denominator.

In this paper we will consider three different experimental schemes: no magnetic field, a weak magnetic field ($g\mu_B B \ll \Delta E_{hf}$), and a strong magnetic field ($g\mu_B B \gg \Delta E_{hf} \gg g_I \mu_N B$). For each we shall calculate the ratio $R = d/\omega\mu$, where d is the PNC E1 amplitude, μ is the M1 amplitude and ω is the transition frequency. A promising transition will have a relatively large R, since the PNC E1 amplitude, d, will be large, the background parity conserving M1 amplitude, μ, will be relatively small, and ideally the transition frequency should also be low, as mentioned previously.

We consider atoms and ions with the electron angular momentum $J = 1/2$. In this case the only allowed values for the total atomic angular momentum are $F = I \pm 1/2$, where I is the nuclear spin. In the presence of a magnetic field, states with a fixed F are split into states with a fixed projection, M, onto the external field direction. The total angular momentum is no longer conserved, there is a mixing of states with the same projection, M, resulting in the appearance of the new states:

$$\begin{aligned} |\Psi^{(1)}, M\rangle &= c_1^{(1)}|I+1/2, M\rangle + c_2^{(1)}|I-1/2, M\rangle \quad (1) \\ |\Psi^{(2)}, M\rangle &= c_1^{(2)}|I+1/2, M\rangle + c_2^{(2)}|I-1/2, M\rangle. \quad (2) \end{aligned}$$

The mixing coefficients, c, in these equations are calculated from the secular equations with the hyperfine interaction and the interaction with the external magnetic field taken together. In the low field limit

$$\begin{aligned} |\Psi^{(1)}, M\rangle &\rightarrow |I+1/2, M\rangle \\ |\Psi^{(2)}, M\rangle &\rightarrow -|I-1/2, M\rangle. \end{aligned}$$

In the high field limit the coupling between I and J is broken and it is no longer proper to consider the states in terms of F, instead we need to consider them in terms of m_I and m_J. In this limit we have the states

$$\begin{aligned} |\Psi^{(1)}, M\rangle &\rightarrow |m_I = M - 1/2, m_J = 1/2\rangle \\ |\Psi^{(2)}, M\rangle &\rightarrow |m_I = M + 1/2, m_J = -1/2\rangle. \end{aligned}$$

It makes no sense to divide the terms into hyperfine and Zeeman transitions in the high field limit because F is not conserved, nevertheless we shall call the $|\Psi^{(1)}\rangle \rightarrow |\Psi^{(2)}\rangle$ transitions the hyperfine ones and the $|\Psi^{(1)}, M\rangle \rightarrow |\Psi^{(1)}, M\pm1\rangle$, and $|\Psi^{(2)}, M\rangle \rightarrow |\Psi^{(2)}, M\pm1\rangle$ the Zeeman ones.

The dependence of the ^{133}Cs $6s_{1/2}$ energy levels on the external magnetic field is presented in Figure 1. In weak magnetic fields the energy difference of the hyperfine term $|\Psi^{(1)}\rangle$ and $|\Psi^{(2)}\rangle$ is constant and equal to ΔE_{hf} while the energy difference of the Zeeman terms is proportional to the field. In the strong field the hyperfine transition energy increases in proportion to the field while the Zeeman transition energy is constant and equal to $\Delta E_{hf}/(2I+1)$. Here and below we neglect small terms $\sim \mu_n B$ where μ_n is the nuclear magnetic moment.

For the hyperfine transitions without the external field the ratio R is given by

$$\begin{aligned} R_0 &= \frac{\langle\Psi^{(2)}, M|d|\Psi^{(1)}, M\rangle}{\omega\langle\Psi^{(2)}, M|\mu|\Psi^{(1)}, M\rangle} \\ &= \left(\frac{I+1/2}{I(I+1)}\right)^{1/2} \frac{\langle I-1/2||d||I+1/2\rangle}{g\mu_B \Delta E_{hf}}. \quad (3) \end{aligned}$$

Here g is the atomic magnetic (Landé) g-factor: $g = 2$ for the $s_{1/2}$ valence electron (K, Rb, Cs, Ba$^+$, Au, Fr), and $g = 2/3$ for the $p_{1/2}$ valence electron (Tl).

In weak fields the E1 amplitudes behave just like the transition frequencies (they are proportional to the field for Zeeman transitions and constant for hyperfine ones), while the M1 amplitudes are independent of the weak field. The R parameters, given by

$$R = \frac{\langle\Psi^{(1)}, M|d_+|\Psi^{(1)}, M+1\rangle}{\omega\langle\Psi^{(1)}, M|\mu_+|\Psi^{(1)}, M+1\rangle},$$

for hyperfine transitions are independent of the field while it is weak. For Zeeman transitions they are given by

$$\begin{aligned} R_{|\Psi^{(1)},M\rangle\rightarrow|\Psi^{(1)},M\pm1\rangle} &= 2IR_0, \quad (4) \\ R_{|\Psi^{(2)},M\rangle\rightarrow|\Psi^{(2)},M\pm1\rangle} &= 2(I+1)R_0. \quad (5) \end{aligned}$$

Here we use spherical components of the electric and magnetic dipole operators defined as $d_+ = (d_x + id_y)/\sqrt{2}$ and $\mu_+ = (\mu_x + i\mu_y)/\sqrt{2}$.

In strong magnetic fields the transitions $|\Psi^{(1)}, M\rangle \rightarrow |\Psi^{(2)}, M \pm 1\rangle$ are not interesting since the transition $|\Psi^{(1)}, M\rangle \rightarrow |\Psi^{(2)}, M+1\rangle$ corresponds to $\Delta I_z = 2$, resulting in the E1 amplitude being forbidden due to selection rules, while for the transition $|\Psi^{(1)}, M\rangle \rightarrow |\Psi^{(2)}, M-1\rangle$ both the M1 and E1 amplitude are independent of the magnetic field and so the magnetic field dependence of R comes entirely from ω which increases linearly with magnetic field, resulting in R decreasing inversely to the magnetic field. By contrast, in the transition $|\Psi^{(1)}, M\rangle \rightarrow |\Psi^{(2)}, M\rangle$ the E1 amplitude is independent of the external magnetic field. The parameter $R_{|\Psi^{(1)},M\rangle\rightarrow|\Psi^{(2)},M\rangle}$ can also be shown to be independent of the field and always equal to R_0. The E1 amplitude of the Zeeman transitions in a strong magnetic field reach a constant value, comparable to the E1 amplitude of the hyperfine transitions. The frequencies also reach a constant value, given by $\omega = \Delta E_{hf}/(2I+1)$, while the M1 transition amplitudes decrease in proportion to the field. This results in the R parameters increasing with the field

$$\begin{aligned} R_{|\Psi^{(1)},M\rangle\rightarrow|\Psi^{(1)},M\pm1\rangle} &= R_{|\Psi^{(2)},M\rangle\rightarrow|\Psi^{(2)},M\pm1\rangle} \\ &= 2(I+1/2)R_0 x, \quad (6) \end{aligned}$$

where $x = g\mu_B B/\Delta E_{hf}$.

Calculated R parameters for a collection of atoms are presented in Table I. In Tables II, III and IV we present ω, d and μ for the different magnetic fields. The dimensionless coupling constant, κ, consisting mainly of the anapole moment of the nucleus has been left as a free parameter, we present an estimate of κ_a in Table III to give an approximation of the size of this term. The P-odd E1 transition amplitudes, d, R parameter and transition frequencies, ω all depend upon the magnetic field, but it is useful to consider d and R as a function of ω. These relationships are presented in Figures 2 and 3. Moving from left to right in these graphs corresponds to an increasing magnetic field. These figures show that for transitions with the same frequency, Zeeman transitions have a larger P-odd E1 amplitude as well as a larger ratio of the E1 amplitude to the P-even M1 amplitude than the hyperfine transitions.

We conclude that Zeeman transitions in heavy atoms have some advantages over the hyperfine transitions that have been considered previously. The biggest advantage is that the transition frequencies can be tuned to make an experiment easier to perform, increase sensitivity and provide additional control of systematic effects by varying the magnetic field. Zeeman transitions should be considered as candidates for experiments to measure the anapole moment of nuclei.

FIG. 1: Zeeman splitting of the hyperfine terms of ^{133}Cs as a function of magnetic field. In weak fields the splitting between hyperfine levels (marked ΔE_{hf}) is fairly constant and the splitting between Zeeman levels increases linearly with the field. In strong fields the splitting between the hyperfine levels increases linearly with the field while the splitting between the Zeeman levels reaches a constant separation (marked ω_Z).

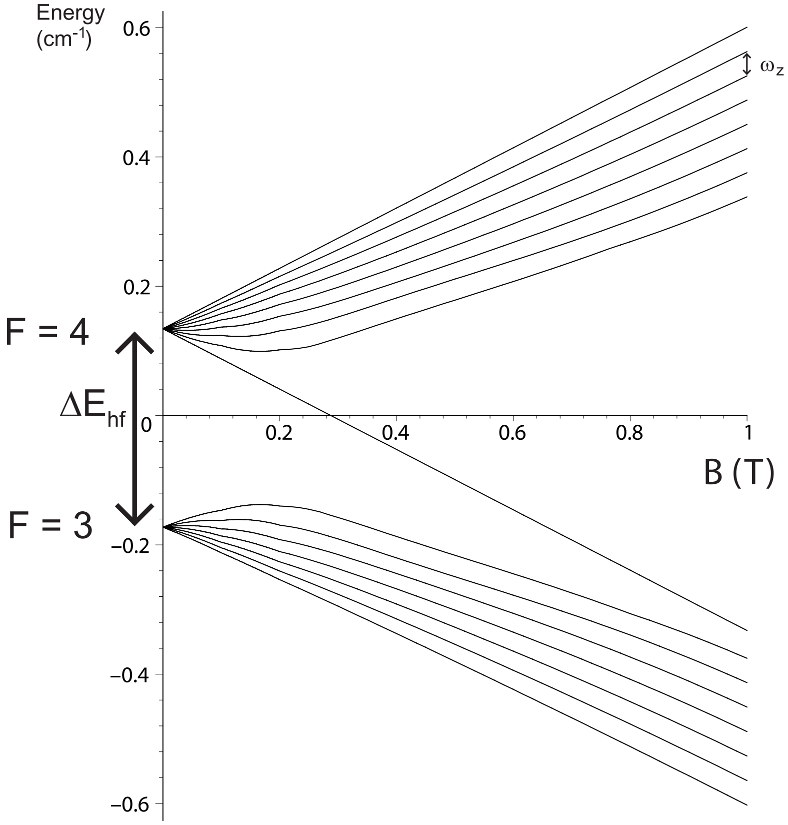

---

[1] J.S.M. Ginges, V.V. Flambaum. Phys. Rep. **397**, 63 (2004).

[2] V. V. Flambaum and I. B. Khriplovich, Sov. Phys. -JEPT **52**, 835 (1980).

[3] C.S. Wood, S.C. Bennet, D. Cho, B.P. Masterson, J.L. Roberts, C.E. Tanner, C.E. Wieman. Science **275**,1759 (1997).

[4] P.A. Vetter, D.M. Meekhof, P.K. Majumder, S.K. Lamoreaux, E.N. Fortson. Phys. Rev. Lett **74**, 2658 (1995).

[5] V. V. Flambaum, I. B. Khriplovich, and O.P. Sushkov. Phys. Lett. B**146**, 367 (1984).

[6] V. V. Flambaum and I. B. Khriplovich, Sov. Phys. -JEPT **62**, 872 (1985).

[7] V. N. Novikov and I. B. Khriplovich, JEPT Lett. **22**, 74 (1975).

[8] V.V. Flambaum, 1987 (unpublished). I.Ya. Kraftmakher. Novosibirsk Institute of Nuclear Physics preprint INP 90-54 (unpublished).

[9] D. Budker, Parity Nonconservation in Atoms, Physics Beyond the Standard Model, Proceedings of the Fifth International WEIN Symposium, P. Herczeg, C. M. Hoffman, and H. V. Klapdor-Kleingrothaus, eds. World Scientific, pp. 418-441 (1999).

[10] V. G. Gorshkov, V. F. Ezhov, M. G. Kozlov, and A. I.

TABLE I: We present the ratio, R, for a range of atoms and ions with J=1/2. R is presented for no magnetic field, a small magnetic field and a large magnetic field, $x = \frac{g\mu_B B}{\Delta E_{hf}}$ is a dimensionless parameter representing the magnetic field strength. The values of the PNC reduced matrix elements, $\langle F_F||d||F_I\rangle$, are taken from [12]. Note that we use the convention for κ and the PNC reduced dipole matrix elements used in the earlier work [2]. To convert to the notation used in [12] κ must be multiplied by the factor $(-1)^{I+1/2+l}\frac{(I+1/2)}{I(I+1)}$ where l is the orbital angular momentum of the unpaired nucleon.

Atom/ion	I	nl	$F_I - F_F$	ΔE_{hf}	$\langle F_F \Vert d \Vert F_I\rangle$	R ($10^{-4} i\kappa Ry^{-1}$)		
				cm^{-1}	$10^{-13} i\kappa e a_B$	$\vert\Psi^{(1)}, M\rangle \to \vert\Psi^{(2)}, M\rangle$	$\vert\Psi^{(1)}, M\rangle \to \vert\Psi^{(1)}, M \pm 1\rangle$	
						$x = 0$	$x \ll 1$	$x \gg 1$
^{39}K	1.5	$4s$	1-2	0.0154[a]	-1.18	-0.85	-2.5	-3.4x
^{85}Rb	2.5	$5s$	2-3	0.101[b]	-8.74	-0.76	-3.8	-4.6x
^{87}Rb	1.5	$5s$	1-2	0.228[c]	7.27	0.35	1.1	1.4x
^{133}Cs	3.5	$6s$	3-4	0.307[a]	-43.8	-1.1	-7.6	-8.6x
^{137}Ba$^+$	1.5	$6s$	1-2	0.268[d]	-32.9	-1.3	-4.0	-5.4x
^{197}Au	1.5	$6s$	1-2	0.203[e]	85.4	4.6	14.	18.x
^{205}Tl	0.5	$6p_{1/2}$	0-1	0.71[f]	-400[h]	-29.	-29.	-59.x
^{211}Fr	4.5	$7s$	4-5	1.451[g]	-481[i]	-2.2	-20.	-22.x

[a] Reference [13]

[b] Reference [14]

[c] Reference [15]

[d] Reference [16]

[e] Reference [17]

[f] Reference [18]

[g] Reference [19]

[h] A significantly different value of -141 was obtained for this reduced matrix element in [20].

[i] A similar value of -445 was calculated in [21].

TABLE II: We present the transition energy (in units cm^{-1}) for the atoms and transitions that have been considered in this paper, $x = \frac{g\mu_B B}{\Delta E_{hf}}$ is a dimensionless parameter related to the magnetic field strength. The $B = 0$ column contains the hyperfine splitting which is referenced in Table I, the next two columns contain the Zeeman splitting between adjacent levels, in cesium these energies correspond to the energy difference marked ω_Z on Fig. 1.

Atom/ion	B=0	$g\mu_B B \ll \Delta E_{hf}$	$g\mu_B B \gg \Delta E_{hf} \gg g_I \mu_N B$
theory	ΔE_{hf}	$\frac{x\Delta E_{hf}}{2I+1}$	$\frac{\Delta E_{hf}}{2I+1}$
^{39}K	0.0154	0.0039x	0.0039
^{85}Rb	0.101	0.0168x	0.0168
^{87}Rb	0.228	0.0570x	0.0570
^{133}Cs	0.307	0.0384x	0.0384
^{137}Ba$^+$	0.268	0.0670x	0.0670
^{197}Au	0.203	0.0508x	0.0508
^{205}Tl	0.71	0.355x	0.355
^{211}Fr	1.451	0.1451x	0.1451

Mikahailov, Sov. J. Nucl. Phys. **48**, 867 (1988).

[11] I. B. Khriplovich, Parity Nonconservation in Atomic Phenomena (Gordon and Breach, New York, 1991).

[12] W. R. Johnson, M. S. Safronova, and U. I. Safronova, Phys. Rev. A **67**, 062106 (2003).

[13] W. Happer, in *Atomic Physics 4*, edited by G. zu Putlitz, E. W. Weber, and A. Winnacker (Plenum Press, New York, 1974), pp. 651-682.

[14] J. Vanier and C. Audoin, The Quantum Physics of Atomic Frequency Standards (Adam Hilgar, Bristol, 1989).

[15] S. Bize *et. al.*, Europhys. Lett. **45**, 558 (1999).

[16] R. Blatt, and G. Werth, Phys. Rev. A **25**, 1476 (1982).

[17] H. Dahman, and S. Penselin, Z. Phys. **200**, 456 (1967).

[18] A. Lurio, and A. G. Prodell, Phys. Rev. **101**, 79 (1956).

[19] S. Liberman *et. al.*, Phys. Rev. A **22**, 2732 (1980).

[20] M. G. Kozlov, JEPT Lett. **75**, 534 (2002).

[21] S. G. Porsev, and M. G. Kozlov, Phys. Rev. A **64**, 064101 (2001).

TABLE III: Here we present the E1 amplitudes as a function of field in units of $i\kappa e a_B$. We include a rough estimate of κ_a. For each atom we present the transition with the largest E1 amplitude in a low field.

Atom/ion	κ_a [a]	$\langle\Psi^{(1)}, M\vert d_z\vert\Psi^{(2)}, M\rangle$ [b] $B = 0$	transition [c]	$\langle\Psi, M+1\vert d_+\vert\Psi, M\rangle$ [d] $g\mu_B B \ll \Delta E_{hf}$	$\langle\Psi, M+1\vert d_+\vert\Psi, M\rangle$ [e] $g\mu_B B \gg \Delta E_{hf} \gg g_I\mu_N B$
^{39}K	0.17	3.7×10^{-14}	I	$2.3 \times 10^{-14}x$	2.7×10^{-14}
^{85}Rb	0.28	2.4×10^{-13}	I	$1.6 \times 10^{-13}x$	1.7×10^{-13}
^{87}Rb	0.28	-2.3×10^{-13}	I	$-1.4 \times 10^{-13}x$	-1.6×10^{-13}
^{133}Cs	0.38	1.1×10^{-12}	I	$7.2 \times 10^{-13}x$	7.6×10^{-13}
^{137}Ba$^+$	0.38	1.0×10^{-12}	I	$6.4 \times 10^{-13}x$	7.4×10^{-13}
^{197}Au	0.49	-2.7×10^{-12}	I	$-1.7 \times 10^{-12}x$	-1.9×10^{-12}
^{205}Tl	0.50	2.3×10^{-11}	II	$1.2 \times 10^{-11}x$	1.6×10^{-11}
^{211}Fr	0.51	1.1×10^{-11}	II	$7.5 \times 10^{-12}x$	7.7×10^{-12}

[a] These are calculated using the formula $\frac{9}{10}\frac{\alpha\mu}{m_p r_0}A^{2/3}g_p$, where α is the fine structure constant, μ is the magnetic moment in nuclear magnetons of the external nucleon (a proton for all the cases above), m_p is the mass of the external nucleon (ie proton mass), $r_0 = 1.2$ fm, and $g_p = 4.5$ is the strength of the weak nuclear potential in units of the Fermi constant G_F. More details about how anapole moments can be calculated can be found in the review [1].

[b] These are calculated using the expression, $-\frac{((I+1/2)^2-M^2)^{1/2}\langle I+1/2\vert\vert d\vert\vert I-1/2\rangle}{2(I(I+1/2)(I+1))^{1/2}}$.

[c] These shows which Zeeman transitions have the largest E1 amplitude in a small field. I stands for the transition $\vert\Psi^{(1)}, -1\rangle \rightarrow \vert\Psi^{(1)}, 0\rangle$ and II stands for the transition $\vert\Psi^{(1)}, 0\rangle \rightarrow \vert\Psi^{(1)}, 1\rangle$. It should be noted that the difference between these amplitudes is very small.

[d] These are calculated using the expression, $-\frac{(I+M+3/2)^{1/2}(I-M+1/2)^{1/2}I^{1/2}\langle I+1/2\vert\vert d\vert\vert I-1/2\rangle}{(I+1)^{1/2}(2I+1)^{3/2}}x$, where $x = \frac{g\mu_B B}{\Delta E_{hf}}$.

[e] These are calculated with the expression, $-\frac{((I+1/2)^2-M^2)^{1/2}\langle I+1/2\vert\vert d\vert\vert I-1/2\rangle}{2(I(I+1)(2I+1))^{1/2}}$.

TABLE IV: Here we present the M1 amplitudes as a function of field in units of $10^{-3}ea_B$. We present the M1 amplitudes for the same transitions as used in Table III.

Atom/ion	$\langle\Psi^{(1)}, M\vert\mu_z\vert\Psi^{(2)}, M\rangle$ [a] $B = 0$	$\langle\Psi, M+1\vert\mu_+\vert\Psi, M\rangle$ [b] $g\mu_B B \ll \Delta E_{hf}$	$\langle\Psi, M+1\vert\mu_+\vert\Psi, M\rangle$ [c] $g\mu_B B \gg \Delta E_{hf} \gg g_I\mu_N B$
^{39}K	-3.2	-2.6	$-2.2/x$
^{85}Rb	-3.4	-2.7	$-2.4/x$
^{87}Rb	-3.2	-2.6	$-2.2/x$
^{133}Cs	-3.5	-2.7	$-2.5/x$
^{137}Ba$^+$	-3.2	-2.6	$-2.2/x$
^{197}Au	-3.2	-2.6	$-2.2/x$
^{205}Tl	-3.6	-1.2	$-0.86/x$
^{211}Fr	-3.6	-2.8	$-2.6/x$

[a] These are calculated using the expression $\frac{-g\mu_B((I+1/2)^2-M^2)^{1/2}}{2I+1}$.

[b] These are calculated using the expression $\frac{-g\mu_B(I+M+3/2)^{1/2}(I-M+1/2)^{1/2}}{\sqrt{2}(2I+1)}$.

[c] These are calculated using the expression $-\frac{((I+1/2)^2-M^2)^{1/2}g\mu_B}{\sqrt{2}(2I+1)x}$ where $x = \frac{g\mu_B B}{\Delta E_{hf}}$.

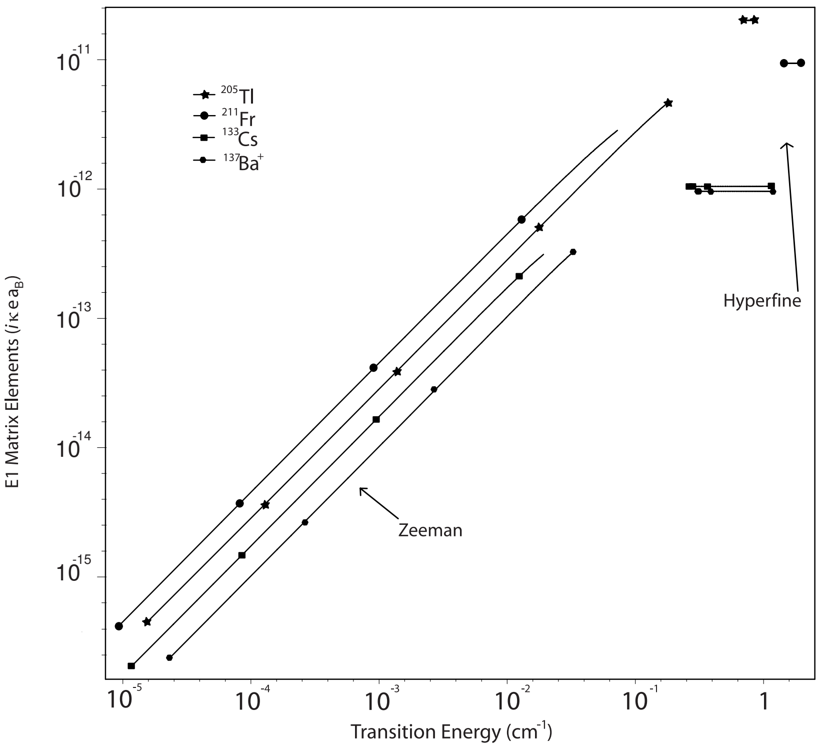

FIG. 2: P-odd E1 transition amplitudes between Zeeman and hyperfine terms of different atoms as a function of transition frequency and external magnetic field. The points represent the elements and also represent the strength of the magnetic field, from left to right 0.0001 T, 0.001 T, 0.01 T, 0.1 T and 1T. The graph shows that the E1 amplitude of Zeeman transitions increases linearly with the field for small fields before reaching a constant value, but retains a constant value for hyperfine transitions, independent of the field. It should be noted that in the case of Zeeman transitions, the transition energy and E1 amplitude reach a constant maximum value at a critical field given by $B = \frac{\Delta E_{hf}}{g\mu_B}$ $(x = 1)$, in this graph the lines for the Zeeman transitions end at half this value $(x = 1/2)$, which is less than 1T for several atoms. The hyperfine transition energy is almost constant for small fields (as can be seen in Fig. 1), resulting in several points appearing at the same position.

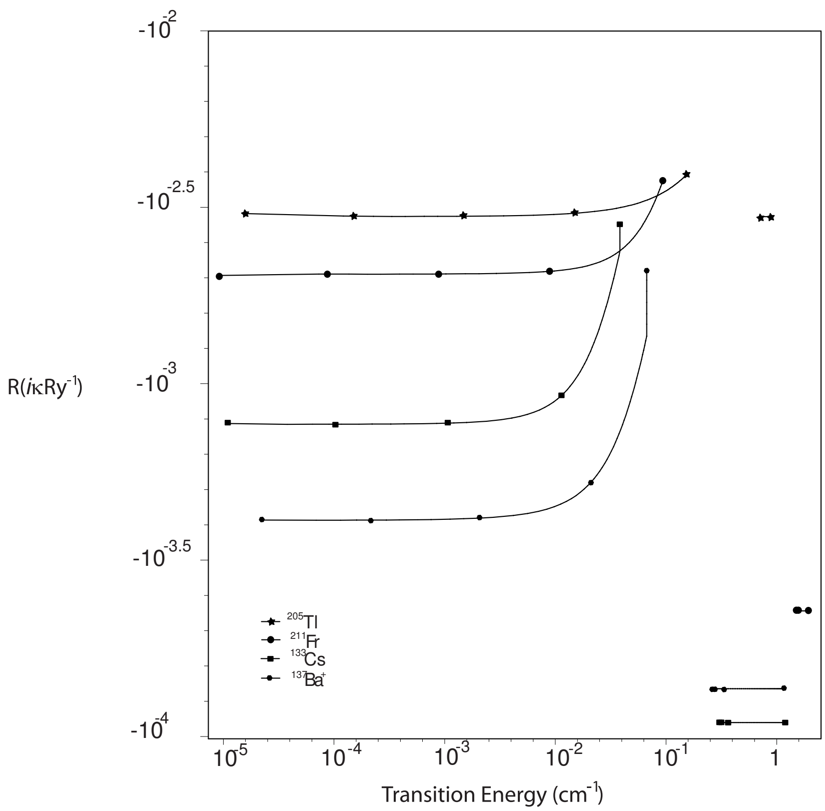

FIG. 3: The ratio, R, of the PNC E1 amplitude, d, to the background $(\omega\mu)$ as a function of external field and transition frequency. The external magnetic field is once again represented by the points, ranging from 0.0001 T up to 1 T from, left to right. This graphs shows that R for Zeeman transitions can be significantly higher than for hyperfine transitions in the same atom.